

DIFFERENTIAL EQUATION BASED FAULT LOCATION ALGORITHM FOR SERIES-COMPENSATED TRANSMISSION LINES

Eugeniusz Rosolowski, Jan Izykowski
 Wrocław University of Technology Wrocław
 Wrocław, Poland
 eugeniusz.rosolowski@pwr.wroc.pl, jan.izykowski@pwr.wroc.pl

Murari Mohan Saha
 ABB Automation Technologies
 Västerås, Sweden
 murari.saha@se.abb.com

Abstract – A new one-end fault location algorithm designated for series-compensated transmission lines is delivered in this paper. It is based on differential equation approach, which allows good reflection of the dynamic phenomena relevant for faults occurring behind the bank of series capacitors (SCs) equipped with metal oxide varistors (MOVs). As a result of that, a good stabilisation of the estimation results (distance to fault, fault path resistance) is assured. This algorithm is recommended for application to the heavy fault cases with high level of noise components in the measured current / voltage signals, which appear as difficult for filtering out with using the earlier known fundamental frequency phasor approach. The algorithm is derived with use of the Clarke transformation for description of the network and the fault. The presented fault location algorithm has been tested and evaluated with use of the ATP-EMTP fault simulation data. The sample results are delivered and discussed.

Keywords: transmission line, series-compensation, MOV, fault location algorithm, differential equation, simulation, ATP-EMTP

1 INTRODUCTION

Use of series capacitor compensation in power transmission line results in achieving the well-known technical and economical benefits. At the same time, series-compensated lines are considered as the power system items, which are extremely difficult for protecting [1]–[5] and for locating faults aimed at the inspection-repair purpose [6]–[8].

In this paper the transmission line compensated with a three-phase capacitor bank installed in the middle (Fig.1a) is considered. Series capacitors (SCs) are equipped for over-voltage protection with non-linear Metal-Oxide Varistors (MOVs) (Fig.1b). Under faults behind SCs&MOVs the fault loop becomes strongly

non-linear, and in consequence the nature of transients, as well as the steady state situation, is entirely different, when comparing with traditional uncompensated lines. It is considered that the fault location is performed prior operation of the thermal protection (TP) at the MOV, which sparks the associated air-gap and thus shunts the MOV.

Faults in series-compensated lines can be located using deterministic [6]–[7] and also using artificial intelligence methods [8]. In [6] the fundamental frequency phasor based fault location algorithm, utilising one-end measurements, has been introduced. SCs&MOVs were equivalented there for the fundamental frequency and the phase co-ordinates approach has been used for formulation of the algorithm. This algorithm is composed of two subroutines, designated for locating faults behind (fault F1 – Fig.1a) and in front of SCs&MOVs (fault F2 – Fig.1a). The final result is obtained by selecting the valid subroutine. The reference [7] deals with application of two-end synchronised measurements for fault location, which appears attractive, however requires the communication means and the GPS.

This paper, as its innovative contribution, delivers the new one-end fault location algorithm, which is based on differential equation approach. The algorithm has been developed with the aim of applying it under heavy fault cases, as the supplementary subroutine to the previous – fundamental frequency phasor approach [6]. This is highly required when a fault appears behind SCs&MOVs (Fig.1a – fault F1) through high fault resistance (considerably above 10Ω) and the fault location is performed from the side of the weak source. Under such faults the measured voltages and currents are grossly contaminated with the components, which are difficult for filtering out with the standard filtering techniques.

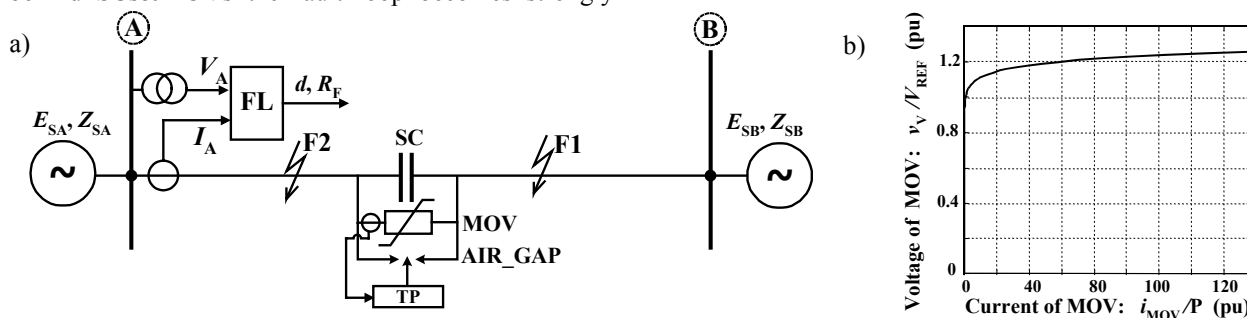


Figure 1: Fault location in series-compensated line: a) schematic diagram, b) voltage-current characteristic of MOV.

The presented fault location algorithm is derived with description of the transmission network for the 0, α , β modes. Application of the generalised fault model, and use of the estimated instantaneous voltage drop across the SC&MOV circuit, are the core of the delivered new fault location algorithm. After derivation of the algorithm, its testing and evaluation with ATP-EMTP fault simulation data follows.

2 FAULT LOCATION ALGORITHM

2.1 Clarke transformation

Transformation of the phase co-ordinates (in time domain) of a 3-phase (a, b, c) symmetrical system into the 0, α , β co-ordinates can be performed according to the following matrix relation:

$$\mathbf{i}_{0\alpha\beta}(t) = \mathbf{C}\mathbf{i}_{abc}(t) \quad (1)$$

where:

$$\mathbf{i}_{0\alpha\beta}(t) = \begin{bmatrix} i_0(t) \\ i_\alpha(t) \\ i_\beta(t) \end{bmatrix}, \quad \mathbf{i}_{abc}(t) = \begin{bmatrix} i_a(t) \\ i_b(t) \\ i_c(t) \end{bmatrix},$$

$$\mathbf{C} = \frac{1}{3} \begin{bmatrix} 1 & 1 & 1 \\ 2 & -1 & -1 \\ 0 & \sqrt{3} & -\sqrt{3} \end{bmatrix}.$$

It is also possible to use the Clarke transformation to phasor representation of a 3-phase system. In this case the instantaneous 0, α , β coordinates can be obtained by taking into account only a real part of the complex transformation.

Considering the phasor representation of currents, the following relations between the Clarke and symmetrical components can be derived:

$$\mathbf{i}_{0\alpha\beta} = \mathbf{C}_s \mathbf{i}_{012} \quad (2)$$

$$\mathbf{i}_{012} = \mathbf{C}_s^{-1} \mathbf{i}_{0\alpha\beta} \quad (3)$$

where:

$$\mathbf{C}_s = \begin{bmatrix} 1 & 0 & 0 \\ 0 & 1 & 1 \\ 0 & -j & j \end{bmatrix}, \quad \mathbf{C}_s^{-1} = \frac{1}{2} \begin{bmatrix} 2 & 0 & 0 \\ 0 & 1 & j \\ 0 & 1 & -j \end{bmatrix}$$

Analogously is for voltages and as a result of that one derives the relation between impedance parameters for the 0, α , β and symmetrical sequences:

$$\begin{aligned} \underline{\mathbf{Z}}_{0\alpha\beta} &= \mathbf{C}_s \underline{\mathbf{Z}}_{012} \mathbf{C}_s^{-1} \\ &= \frac{1}{2} \begin{bmatrix} 2\underline{Z}_0 & 0 & 0 \\ 0 & \underline{Z}_1 + \underline{Z}_2 & j(\underline{Z}_1 - \underline{Z}_2) \\ 0 & -j(\underline{Z}_1 - \underline{Z}_2) & \underline{Z}_1 + \underline{Z}_2 \end{bmatrix} \end{aligned} \quad (4)$$

The transmission network is a static network (positive and negative sequence parameters are identical: $\underline{Z}_1 = \underline{Z}_2$) and therefore one gets that impedance parameters for the 0, α , β and symmetrical sequences are respectively equal to each other:

$$\{\underline{Z}_0\}_{0\alpha\beta} = \{\underline{Z}_0\}_{012}, \quad \underline{Z}_\alpha = \underline{Z}_1, \quad \underline{Z}_\beta = \underline{Z}_1 \quad (5)$$

2.2 Description of the transmission network for 0, α , β modes

Taking into account the above considerations with respect to the Clarke transformation (5) one can represent the transmission network with the series-compensated line as depicted in Fig.2. The equivalent diagram from Fig.2 is valid for each of 0, α , β modes.

It assumed in Fig.2 that the SCs&MOV's banks are installed at distance p (pu) from the terminal A. The respective voltage drops across the SCs&MOV's (V_V) for particular 0, α , β modes represent the banks. These voltage drops are obtained from the instantaneous voltage drops, which in this study are considered as estimated by solving the non-linear differential equation stated for the SC&MOV circuit [3].

The respective resistances and inductances represent the transmission line (note: shunt parameters of the line are not taken into account at this stage). The respective impedance parameters and the EMFs represent the equivalent systems behind the line terminals. For the balanced 3-phase sources their representation for the 0 mode involves the EMF equal to zero.

2.3 Generalised fault loop model

A generalised model of the fault loop considered for different fault types can be described in the similar way as for the symmetrical components [9]. Taking the Laplace transformation (s - Laplace operator) one obtains the following fault loop model:

$$\begin{aligned} V_{A_p}(s) - dZ_{1L}(s)I_{A_p}(s) - V_{V_p}(s) \\ - R_F(a_{F0}I_{F0}(s) + a_{F\alpha}I_{F\alpha}(s) + a_{F\beta}I_{F\beta}(s)) = 0 \end{aligned} \quad (6)$$

where:

d - unknown and sought distance to fault (pu),

$Z_{1L}(s) = R_{1L} + sL_{1L}$, R_{1L} , L_{1L} - positive sequence resistance and inductance of the faulted line,

$V_{A_p}(s)$, $I_{A_p}(s)$ - fault loop voltage and current, composed according to the fault type,

$V_{V_p}(s)$ - voltage drop across SC&MOV circuit for the considered fault loop (single phase or inter-phase loop),

R_F - fault resistance,

$I_{Fi}(s)$ - sequence components of the total fault current ($i = 0$ - zero, $i = 1$ - positive, $i = 2$ - negative sequences),

a_{Fi} - share coefficients dependent on fault type.

Fault loop voltage and current from (6) are determined in the following way:

$$V_{A_p}(s) = a_0V_{A_0}(s) + a_\alpha V_{A_\alpha}(s) + a_\beta V_{A_\beta}(s) \quad (7)$$

$$I_{A_p}(s) = a_0 \frac{Z_{0L}(s)}{Z_{1L}(s)} I_{A_0}(s) + a_\alpha I_{A_\alpha}(s) + a_\beta I_{A_\beta}(s) \quad (8)$$

The weighting coefficients a_0 , a_α , a_β in (7)–(8) and the share coefficients a_{F0} , $a_{F\alpha}$, $a_{F\beta}$ from (6) have to be determined in such a way that they take the real number values, what facilitates the algorithm formulation. Using the transformation rules (2)–(3) one deter-

mines their values, which are gathered in Table 1 and Table 2.

The share coefficients for 0, α , β modes can be determined as follows:

$$a_{F0} = \underline{a}_{F0} \quad (9)$$

$$\underline{a}_{F\alpha} = 0.5(\underline{a}_{F1} + \underline{a}_{F2}) \quad (10)$$

$$\underline{a}_{F\beta} = 0.5 j(\underline{a}_{F1} - \underline{a}_{F2}) \quad (11)$$

There is some freedom in selecting the share coefficients [9]. In order to get the share coefficients (9)–(11) as real numbers special set of these coefficients for the symmetrical components has been selected (Table 2). This was obtained from analysis of the boundary conditions of faults.

Next step in the derivation of the fault location algorithm is related with determination of the total fault current components for the respective 0, α , β modes. This requires considering the flow of fault currents in the circuits for particular 0, α , β modes (Fig.3 shows this circuit for the α mode). As a result of that one obtains:

$$I_{F\alpha}(s) = \frac{\Delta I_{A\alpha}(s)}{k_{F\alpha}(s)} + \frac{\Delta V_{V\alpha}(s)}{Z_{\Delta V\alpha}(s)} \quad (12)$$

$$I_{F\beta}(s) = \frac{\Delta I_{A\beta}(s)}{k_{F\beta}(s)} + \frac{\Delta V_{V\beta}(s)}{Z_{\Delta V\beta}(s)} \quad (13)$$

$$I_{F0}(s) = \frac{I_{A0}(s)}{k_{F0}(s)} + \frac{\Delta V_{V0}(s)}{Z_{\Delta V0}(s)} \quad (14)$$

where:

$I_{F0}(s)$, $I_{F\alpha}(s)$; $I_{F\beta}(s)$ – 0, α , β components of the total fault current,

$k_{F0}(s)$, $k_{F\alpha}(s)$, $k_{F\beta}(s)$ – fault current distribution factors for particular modal quantities,

$I_{A0}(s)$, $\Delta I_{A\alpha}(s) = I_{A\alpha}(s) - I_{A\alpha_pre}(s)$ and

$\Delta I_{A\beta}(s) = I_{A\beta}(s) - I_{A\beta_pre}(s) - 0$, α , β components of currents measured at the terminal A,

$V_{V0}(s)$, $\Delta V_{V\alpha}(s) = V_{V\alpha}(s) - V_{V\alpha_pre}(s)$ and

$\Delta V_{V\beta}(s) = V_{V\beta}(s) - V_{V\beta_pre}(s) - 0$, α , β components of incremental voltage drop across the SC&MOV, as seen from the station A;

$Z_{\Delta V0}(s)$, $Z_{\Delta V\alpha}(s)$, $Z_{\Delta V\beta}(s)$ – impedance of the equivalent circuit, which reflects participation of the adequate voltage components: $\Delta V_{V0}(s)$, $\Delta V_{V\alpha}(s)$ and $\Delta V_{V\beta}(s)$ in particular components of the total fault current.

Note that in cases of the α and β modes the superimposed (incremental) quantity (post-fault current minus pre-fault quantity) is used.

Fault current distribution factors and mentioned impedances of the equivalent circuits depend on the configuration of the transmission network (Fig.3) and impedance parameters. Assuming that all impedances for the positive and for the negative sequence are equal to each other, one obtains analogously as for the symmetrical components approach:

$$k_{F\alpha}(s) = k_{F\beta}(s) = \frac{dK_1(s) + L_1(s)}{M_1(s)} \quad (15)$$

$$Z_{\Delta V\alpha}(s) = Z_{\Delta V\beta}(s) = \frac{dK_1(s) + L_1(s)}{N_1(s)} \quad (16)$$

Coefficients, which are used for composing the fault current distribution factor (15) and impedance of the equivalent circuit (16) are gathered in Table 3. The case of a single (Fig.3) line has been considered for that. Parameters for the zero sequence circuit are not considered here because the share coefficient for the zero sequence and thus for the 0 mode equals zero.

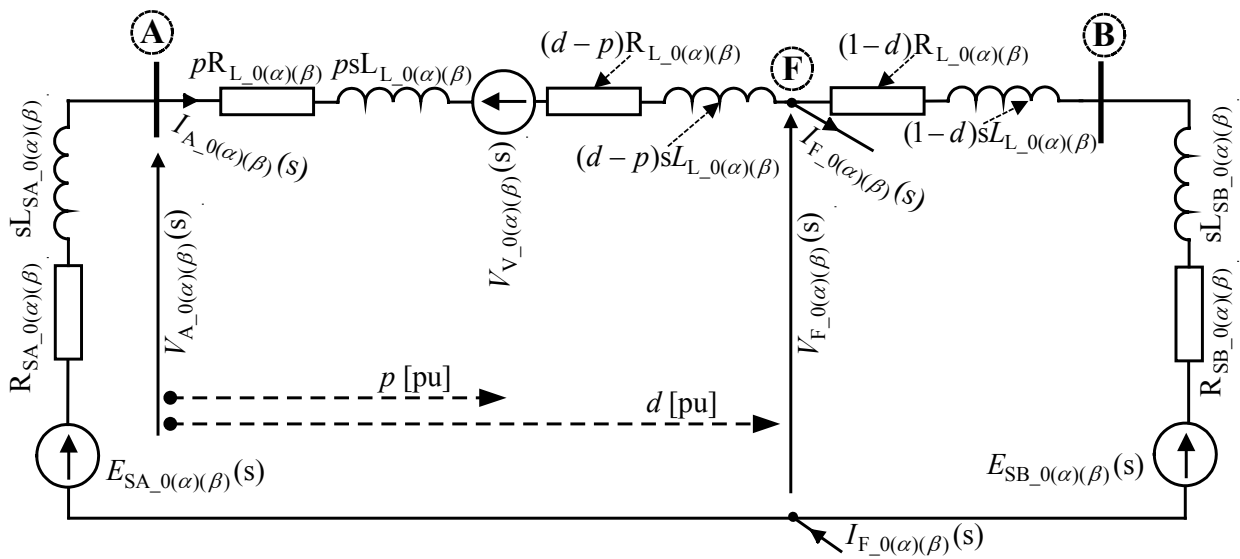


Figure 2: Equivalent circuit diagram of the investigated transmission network for 0, α , β components.

Fault type	Symmetrical components			α, β components; note: $a_0 = \underline{a}_0$	
	\underline{a}_0	\underline{a}_1	\underline{a}_2	a_α	a_β
a-g	1	1	1	1	0
b-g	1	\underline{a}^2	\underline{a}	-0.5	$0.5\sqrt{3}$
c-g	1	\underline{a}	\underline{a}^2	-0.5	$-0.5\sqrt{3}$
a-b, a-b-g a-b-c, a-b-c-g	0	$1 - \underline{a}^2$	$1 - \underline{a}$	1.5	$-0.5\sqrt{3}$
b-c, b-c-g	0	$\underline{a}^2 - \underline{a}$	$\underline{a} - \underline{a}^2$	0	$\sqrt{3}$
c-a, c-a-g	0	$\underline{a} - 1$	$\underline{a}^2 - 1$	-1.5	$-0.5\sqrt{3}$
$\underline{a} = \exp(j2\pi/3)$					

Table 1: Composition of fault loop signals for symmetrical components and 0, α, β components.

Fault type	Symmetrical components			α, β components; note: $a_{F0} = \underline{a}_{F0}$	
	\underline{a}_{F0}	\underline{a}_{F1}	\underline{a}_{F2}	$a_{F\alpha}$	$a_{F\beta}$
a-g	0	1.5	1.5	1.5	0
b-g	0	$1.5 \underline{a}^2$	$1.5 \underline{a}$	-0.75	$0.75\sqrt{3}$
c-g	0	$1.5 \underline{a}$	$1.5 \underline{a}^2$	-0.75	$-0.75\sqrt{3}$
a-b	0	$0.5(1 - \underline{a}^2)$	$0.5(1 - \underline{a})$	0.75	$-0.25\sqrt{3}$
b-c	0	$0.5(\underline{a}^2 - \underline{a})$	$0.5(\underline{a} - \underline{a}^2)$	0	$0.5\sqrt{3}$
c-a	0	$0.5(\underline{a} - 1)$	$0.5(\underline{a}^2 - 1)$	-0.75	$-0.25\sqrt{3}$
a-b-g	0	$1 - \underline{a}^2$	$1 - \underline{a}$	1.5	$-0.5\sqrt{3}$
b-c-g	0	$\underline{a}^2 - \underline{a}$	$\underline{a} - \underline{a}^2$	0	$\sqrt{3}$
c-a-g	0	$\underline{a} - 1$	$\underline{a}^2 - 1$	-1.5	$-0.5\sqrt{3}$
a-b-c-g, a-b-c	0	$1 - \underline{a}^2$	$1 - \underline{a}$	1.5	$-0.5\sqrt{3}$

Table 2: Sets of the weighting coefficients for determining the voltage drop across the fault path resistance.

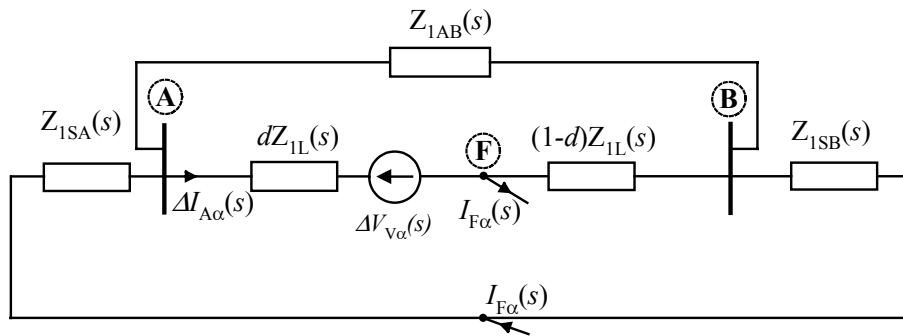


Figure 3: Circuit diagram for α mode for consideration of fault currents flow.

$Z_{1AB}(s) \neq \infty$	$K_1(s) = -Z_{1L}(s)Z_{1AB}(s) - (Z_{1sA}(s) + Z_{1sB}(s))Z_{1L}(s)$ $L_1(s) = Z_{1L}(s)(Z_{1sA}(s) + Z_{1sB}(s)) + Z_{1AB}(s)(Z_{1L}(s) + Z_{1sB}(s))$ $M_1(s) = (Z_{1sA}(s) + Z_{1sB}(s))(Z_{1AB}(s) + Z_{1L}(s)) + Z_{1L}(s)Z_{1AB}(s)$ $N_1(s) = Z_{1sA}(s) + Z_{1sB}(s) + Z_{1AB}(s)$
$Z_{1AB}(s) \rightarrow \infty$	$K_1(s) = -Z_{1L}(s) \quad L_1(s) = Z_{1L}(s) + Z_{1sB}(s)$ $M_1(s) = Z_{1sA}(s) + Z_{1sB}(s) + Z_{1L}(s) \quad N_1(s) = 1$

Table 3: Coefficients used for composing fault current distribution factors.

After introducing the fault current distribution factors (15)–(16) into the generalized fault loop model (1) the quadratic formula with two unknowns (d (pu) – sought fault distance, R_F – fault resistance) is obtained:

$$A(s)d^2 - B(s)d + C(s) - R_F D(s) = 0 \quad (9)$$

where:

$$\begin{aligned} A(s) &= -K_1(s)Z_{1L}(s)I_{A_p}(s), \\ B(s) &= \left(L_1(s)Z_{1L}(s)I_{A_p}(s) - K_1(s)(V_{A_p}(s) - V_{V_p}(s)) \right), \\ C(s) &= L_1(s)(V_{A_p}(s) - V_{V_p}(s)), \\ D(s) &= M_1(s)(a_{F\alpha}\Delta I_{A\alpha}(s) + a_{F\beta}\Delta I_{A\beta}(s)) \\ &\quad + N_1(s)(a_{F\alpha}\Delta V_{V\alpha}(s) + a_{F\beta}\Delta V_{V\beta}(s)) \end{aligned}$$

Then, the bilinear transformation is used for transforming (9) from the Laplace (s) domain into the discrete time (k) domain:

$$s = m_s \frac{1 - z^{-1}}{1 + z^{-1}} \quad (11)$$

where:

$$m_s = \frac{\omega_1}{\tan(0.5\omega_1 T_s)},$$

T_s – sampling period, ω_1 – angular frequency.

Application of (11) yields:

$$A(k)d^2 - B(k)d + C(k) - R_F D(k) = 0 \quad (12)$$

The coefficients involved in (12) are determined by the network parameters, three consecutive samples of the measured signals and three consecutive samples of the estimated voltage drop across the SC&MOV [9].

The coefficients of (12) were orthogonalised with the half-cycle Fourier algorithm and then the formula (12) was solved as for the phasor-based approach. Because of transients in the measured signals, the obtained results exhibit extensive fluctuations. Therefore, for stabilisation of the final result the half-period (processing $N/2$ samples) mean value filter was applied. The recursive form of such a filter for a distance to fault (analogously is for a fault resistance) is as follows:

$$d_f(k) = d_f(k-1) + \frac{2}{N}(d(k) - d(k - N/2)) \quad (13)$$

The other possibility of smoothing results can also be considered for that, as for example use of median filters.

3 ATP-EMTP EVALUATION

The presented fault location algorithm has been evaluated with using the fault data obtained from ATP-EMTP [10] versatile simulations of faults. The studied network contains the 400 kV, 300 km transmission line, compensated at 70% rate. The parameters of the network are gathered in Table 4. Capacitive voltage transformers (CVTs) and current transformers (CTs) have been modelled together with the second order analogue anti-aliasing filters with the cut-off frequency set to 350 Hz. Signals were sampled at 1000 Hz.

Different specifications of faults have been considered in the study. Selected results are depicted in Fig.4–Fig.5.

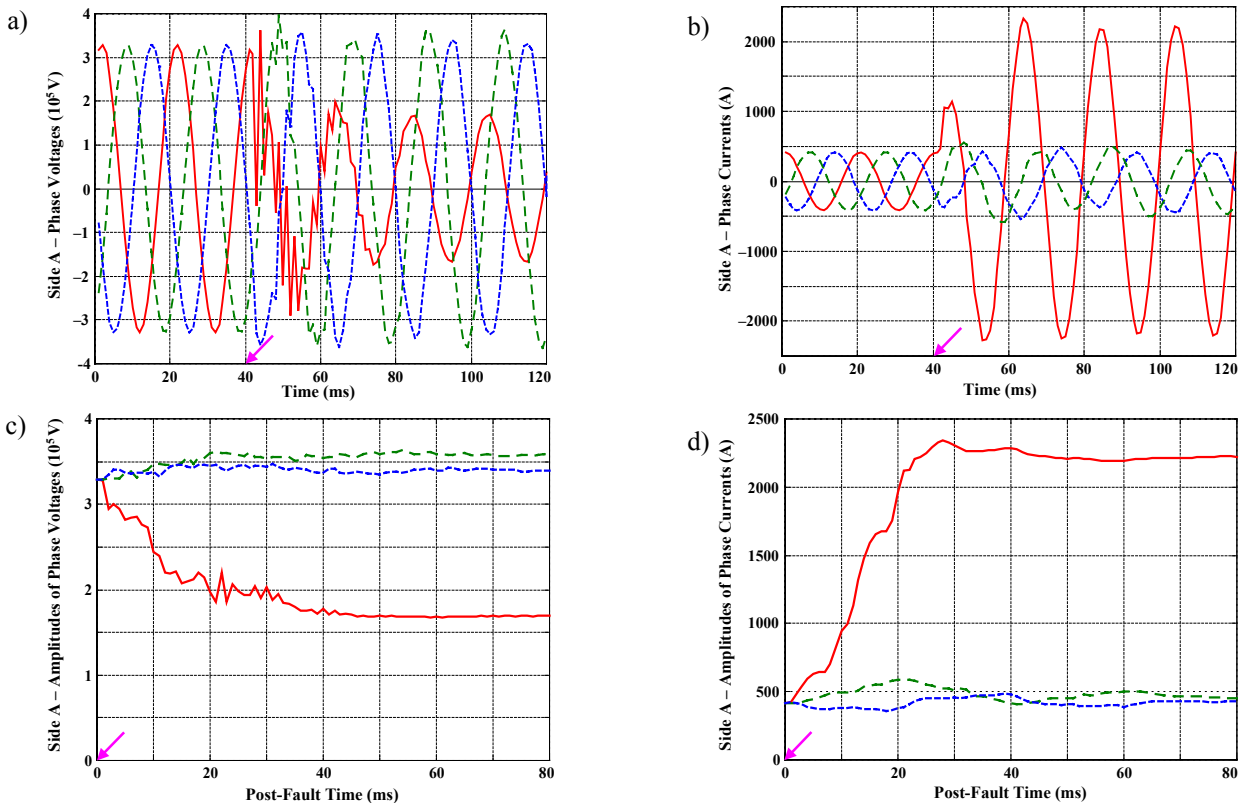


Figure 4: Example of heavy fault location: a) phase voltages, b) phase currents, c) amplitudes of voltages, d) amplitudes of currents.

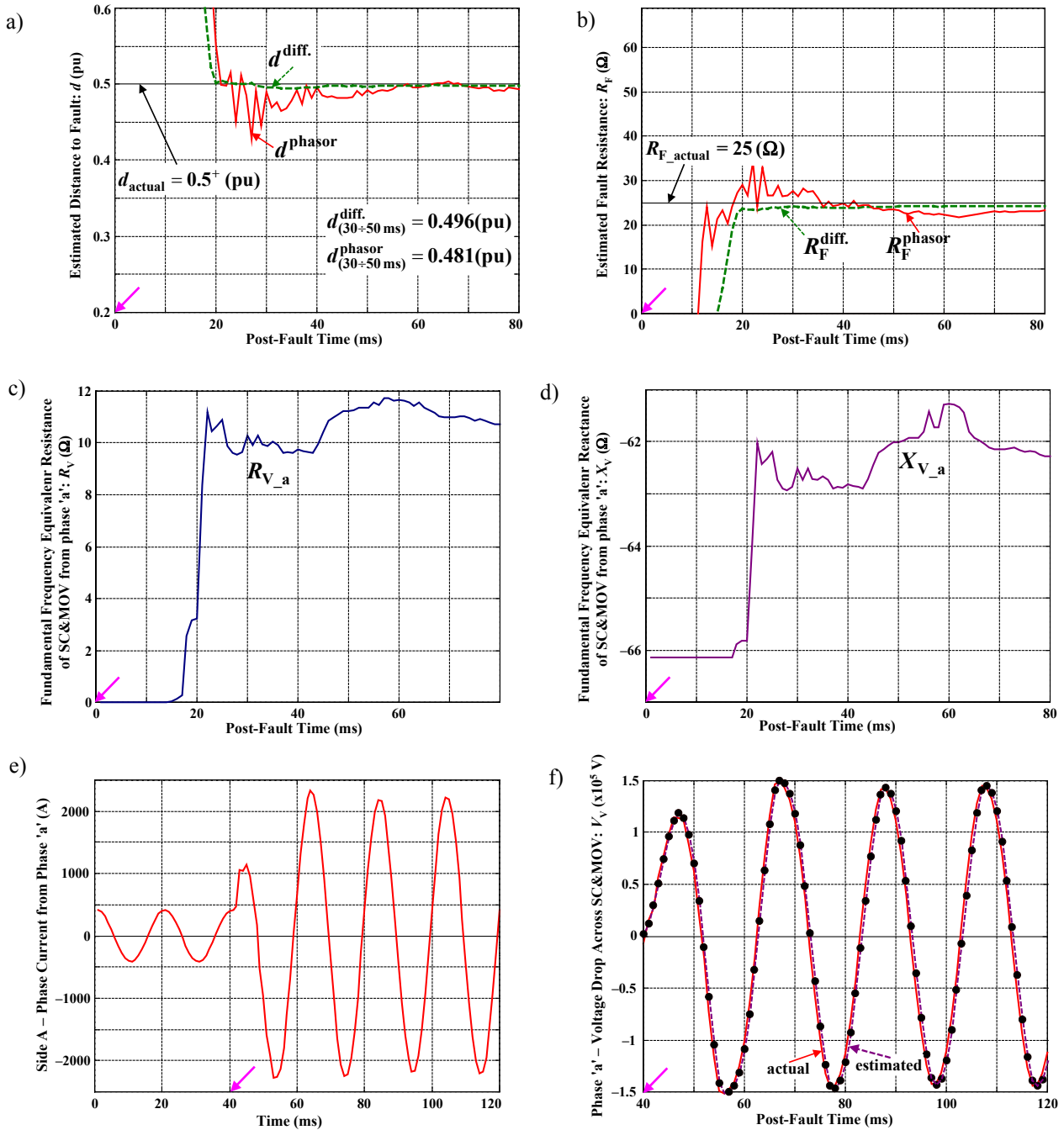


Figure 5: Example of heavy fault location: a) estimated distance to fault, b) estimated fault resistance, c) estimated equivalent fundamental frequency resistance, d) estimated equivalent fundamental frequency reactance, e) input signal of the procedure for estimation of SC&MOV voltage drop, f) output signal of the procedure for estimation of SC&MOV voltage drop .

The simulation case, for which the results are presented in Fig.4 – Fig.5 has the following specifications: a–g fault at distance 0.5^+ (pu), i.e. just behind SCs&MOVs, fault resistance $R_F = 25\Omega$, fault location: performed from the terminal A (weak equivalent system behind this terminal – Table 4). Waveforms of the fault locator input voltage (Fig.4a) and current (Fig. 4b) for this case are contaminated with components difficult for filtering out. As a result of that one observes rather pure stabilisation of the signals amplitudes (Fig.4c, Fig.4d), calculated with use of the standard full-cycle Fourier technique.

Fig.5a – Fig.5b present the estimation results. The results obtained with the earlier method, i.e. with the fundamental frequency phasor based approach [6]: d^{phasor} , R_F^{phasor} exhibit some transients. The fault location error is around 2%. In contrast, for the results obtained with use of the method delivered in this paper, i.e. with the differential equation based approach: d^{diff} , R_F^{diff} very good stabilisation is observed. The fault location error is below 0.5%.

Fig.5c – Fig.5d show the fluctuations in the fundamental frequency equivalent of SCs&MOV [6]: resis-

tance (R_{V_a}) and reactance (X_{V_a}) from the faulted phase. These fluctuations show how the considered fault case is difficult for the location.

Fig.5e – Fig.5f show the input signal (measured current) and the output of the procedure [3] (estimated voltage drop across the SC&MOV), which is used for determining the representation of the capacitor bank used in the presented technique. The estimated drop (Fig.5f – dashed line with the calculations points marked by dots) accurately follows the actual voltage drop (solid line).

Component	Parameter	
Line AB	ℓ	300 km
	Z'_{1L}	(0.0276+0.3151) Ω /km
	Z'_{0L}	(0.2750+1.0265) Ω /km
	C'_{1L}	13.0 nF/km
	C'_{0L}	8.5 nF/km
Series capacitors	X_C	0.70 X_{1L}
	p	0.5 pu
MOVs characteristic: $i_{MOV} = P \left(\frac{v_V}{V_{REF}} \right)^q$	P	1 kA
	V_{REF}	150 kV
	q	23
Equivalent system at terminal A	Z_{1SA}	(8.0+j100.0) Ω
	Z_{0SA}	(14.0+j150.0) Ω
	Angle of EMFs	0 deg
Equivalent system at terminal B	Z_{1SB}	(1.312+j15) Ω
	Z_{0SB}	(2.334+j26.6) Ω
	Angle of EMFs	-30 deg

Table 4: Parameters of the transmission network.

4 CONCLUSIONS

In the paper the new accurate algorithm for locating faults on power transmission line with series capacitor compensation has been delivered. The algorithm allows achieving good stabilization of the estimation results for the heavy fault cases with grossly contaminated the fault locator input signals. Such cases happen for faults behind SCs&MOVs with involving high fault resistance, especially if the location is performed from the weak equivalent system side.

The delivered fault location algorithm imposes higher computational burden than the previous phasor based approach. However, this can be accepted since the computations are to be performed in the off-line regime.

Innovative contribution of this paper relies on:

- the dynamic behaviour of SCs&MOVs has been accounted for by representing them with the estimated voltage drops across the capacitor banks,
- inclusion of such representation of SCs&MOVs has become possible with the derived differential equation based fault location algorithm

–use of the Clarke transformation together with the general fault loop model has allowed to get the algorithm in which the measured signals are processed in a convenient way, i.e. with use only real number coefficients.

The performed testing and evaluation with the fault data obtained from ATP-EMTP simulations proved superior (in comparison to the previous approach) performance of the presented fault location algorithm under heavy fault cases.

REFERENCES

- [1] F. Ghassemi, J. Goodarzi and A.T. Johns, "Method to improve digital distance relay impedance measurement when used in SC lines protected by a metal oxide varistor", IEE Proc. Transm. Distrib., vol. 145, No. 4, pp. 403–408, July 1998
- [2] J.A.S.B. Jayasinghe, R.K. Aggarwal, A.T. Johns and Z.Q. Bo, "A novel non-unit protection for series compensated ehv transmission lines based on fault generated high frequency voltage signals", IEEE Trans. on Power Delivery, Vol.13, No.2, pp.405–413, 1998
- [3] M.M. Saha, B. Kasztenny, E. Rosolowski and J. Izykowski, "First zone algorithm for protection of series compensated lines", IEEE Trans. on Power Delivery, Vol.16, No.2, pp. 200–207, 2001
- [4] B. Kasztenny, "Distance protection of series compensated lines – problems and solutions", Proceedings of 28th Annual western Protective Relay Conference, Spokane, USA, pp. 1–34, 2001
- [5] M.El. Erezzaghi, P.A. Crossley and R. Elferes, "Design and evaluation of an adaptive distance protection scheme suitable for series compensated transmission feeders", Proceedings of Developments in Power System Protection, Amsterdam, pp. 454–456, 2004
- [6] M.M. Saha, J. Izykowski, E. Rosolowski and B. Kasztenny, "A new accurate fault locating algorithm for series compensated lines", IEEE Trans. on Power Delivery, vol. 14, No.3, pp. 789–795, 1999
- [7] Chi-Shan Yu, Chih-Wen Liu, Sun-Li Yu and Joe-Air Jiang, "A new PMU-based fault location algorithm for series compensated lines", IEEE Trans. on Power Delivery, Vol. 17, No. 1, pp. 33–46, January 2002
- [8] D. Novosel, B. Bachmann, D. Hart, Y. Hu and M.M. Saha, "Algorithms for locating faults on series compensated lines using neural network and deterministic methods", IEEE Trans. on Power Delivery, Vol. 11, No. 4, pp. 1728–1736, 1996
- [9] J. Izykowski, E. Rosolowski, M.M. Saha, "Locating faults in parallel transmission lines under availability of complete measurements at one end", IEE Gener., Transm. and Distrib., Vol. 151, No. 2, pp. 268-273, March 2004
- [10] H. Dommel, "Electro-Magnetic Transients Program", BPA, Portland, Oregon, 1986.